Agrobacterium-mediated *Cuscuta campestris* transformation as a tool for understanding plant-plant interactions

Supral Adhikari[1, †], Asha Mudalige[1, †], Lydia Phillips[1], Hyeyoung Lee[2], Vivian Bernal-Galeano[3], Hope Gruszewski[3], James H. Westwood[3], So-Yon Park*[1]

[1] Division of Plant Science and Technology, University of Missouri, Columbia, MO, 65211, USA

[2] Division of Animal Science, University of Missouri, Columbia, MO, 65211, USA

[3] School of Plant and Environmental Sciences, Virginia Tech, Blacksburg, VA, 24061, USA

*Author for correspondence: parksoy@missouri.edu

[†] These authors contributed equally to this article.

ORCIDs:

Supral Adhikari https://orcid.org/0000-0002-9914-2986

Asha Mudalige https://orcid.org/0009-0002-2842-1758

Lydia Phillips

Hyeyoung Lee

Vivian Bernal-Galeano https://orcid.org/0000-0002-0438-2937

Hope Gruszewski

James H. Westwood https://orcid.org/0000-0001-5127-7294

So-Yon Park https://orcid.org/0000-0002-2126-3382

Summary

Cuscuta campestris, a stem parasitic plant, has served as a valuable model plant for the exploration of plant-plant interactions and molecular trafficking. However, a major barrier to *C. campestris* research is that a method to generate stable transgenic plants has not yet been developed. Here, we describe the development of a *Cuscuta* transformation protocol using various reporter genes (GFP, GUS, or RUBY) and morphogenic genes (*CcWUS2* and *CcGRF/GIF*), ultimately leading to a robust protocol for *Agrobacterium*-mediated *C. campestris* transformation. The stably transformed and regenerated RUBY *C. campestris* plants produced haustoria, the signature organ of parasitic plants, and these were functional in forming host attachments. The locations of T-DNA integration in the parasite genome were confirmed through TAIL-PCR. Transformed *C. campestris* also produced flowers and transgenic seeds exhibiting betalain pigment, providing proof of germline transmission of the RUBY transgene. Furthermore, the RUBY reporter is not only a useful selectable marker for the *Agrobacterium*-mediated transformation, but also provides insight into the movement of molecules from *C. campestris* to the host during parasitism. Thus, the protocol for transformation of *C. campestris* reported here overcomes a major obstacle to *Cuscuta* research and opens new possibilities for studying parasitic plants and their interactions with hosts.

Key words: *Cuscuta*, parasitic plant, *Agrobacterium*-mediated transformation, plant-plant interactions, RUBY, mobile molecules.

Introduction

Cuscuta spp. are obligate stem parasitic plants that infect a broad range of host plants (Dawson *et al.*, 1994). The thread-like plant consists of leafless, twining stems that can attach to aerial parts of herbaceous plants, woody shrubs, and even trees. The parasitic invasion of *Cuscuta* begins by coiling around the stem of its host plant and initiating points of growth toward the host. The epidermal cells of these adhesive disk structures secrete a bioadhesive substance that anchors the parasite to the host (Vaughn, 2002; Galloway *et al.*, 2020). Next, a multicellular feeding structure termed the haustorium develops from the parasite stem and breaches the host tissues using a combination of mechanical pressure and enzymatic digestion of host cell walls, ultimately resulting in vascular connections with the host (Nagar *et al.*, 1984; Johnsen *et al.*, 2015; Kaiser *et al.*, 2015).

Cuscuta spp. are among the most agriculturally destructive parasitic weeds, as well as interesting subjects for studies of plant-plant interaction. The economic impact is due to their wide range of potential host species, which includes many dicotyledonous crops and ornamental plants (Lanini & Kogan, 2005), as well as their habit of extracting water and nutrients that the host needs for productivity. For example, *C. campestris* reduced tomato fresh weight by 98% in a greenhouse study (Goldwasser *et al.*, 2012), and *C. indecora* decreased alfalfa yield by 57% (Cudney *et al.*, 1992). Although cultural, chemical, and mechanical control methods have been developed to suppress the growth of *Cuscuta*, there is currently no efficient method to eliminate established *Cuscuta* without also causing damage to their hosts (Dechassa & Regassa, 2021).

Cuscuta spp. are useful for plant biology because their parasitic lifestyle provides insights into the mechanisms by which plants detect and interact with other plants. Examples of this include *Cuscuta* detection of neighboring plants by volatile signals (Runyon *et al.*, 2006), *Cuscuta*-to-host bidirectional mobility of mRNAs, small RNAs, and proteins (Kim *et al.*, 2014; Shahid *et al.*, 2018; Liu *et al.*, 2020; Park *et al.*, 2022), and elucidation of host resistance mechanisms against parasites (Hegenauer *et al.*, 2016; Hegenauer *et al.*, 2020). Therefore, both applied and basic plant sciences would benefit from greater ability to investigate the molecular mechanisms underlying interactions between *Cuscuta* spp. and *their* hosts.

Plant genetic transformation is an essential tool for functional genomic studies as it enables the manipulation of gene expression through the creation of knockout or overexpression mutant lines. This approach has been used for selected species of parasitic plants in the family

Orobanchaceae to understand the mechanisms by which they develop and interact with their hosts. Methods for the transient and stable transformation of these root parasitic plants have been published for *Triphysaria versicolor, Phtheirospermum japonicum*, and *Phelipanche aegyptiaca* (Tomilov *et al.*, 2007; Fernández-Aparicio *et al.*, 2011; Ishida *et al.*, 2011; Bandaranayake & Yoder, 2018).

As for *Cuscuta* transformation, several efforts have led to partial success. Regeneration of shoots from callus of *C. reflexa* (Srivastava & Dwivedi, 2001) has been reported, and transformation was accomplished in cultured *C. trifolii* (Borsics *et al.*, 2002) and *C. europeae* (Švubová & Blehová, 2013). Transformation of haustorial structures was recently accomplished in *C. reflexa* (Lachner *et al.*, 2020). However, despite these attempts with diverse *Cuscuta* species, the inability to regenerate a functional *Cuscuta* plant from transformed explant tissues has blocked progress toward achieving stably transformed *Cuscuta*.

The failure to regenerate plants from transgenic callus is a common bottleneck in plant transformation, but progress has come from the use of genes involved in morphogenesis, which promote the formation of plant organs in callus of plant species that are recalcitrant to transformation or regeneration (Lee & Wang, 2023). For example, recent reports have shown improved regeneration and transformation efficiency in maize (*Zea maize*) with morphogenic transcription factors such as *WUSCHEL* (*WUS*) and *BABY BOOM* (*BBM*). *WUS*, previously known to play a vital role in maintaining the stem cell population, was also found to enhance embryogenesis in *Arabidopsis* (Zuo *et al.*, 2002). When used with a transformation recalcitrant maize line, *BBM-WUS* enhanced transformation efficiency by over 40% (Lowe *et al.*, 2016). In another approach, a chimera consisting of *GROWTH-REGULATING FACTOR* (*GRF*) and its co-factor *GRF-INTERACTING FACTOR* (*GIF*) was shown to promote transformation and regeneration efficiency in wheat (*Triticum aestivum*) and citrus (*Citrus sinensis Osb.* × *Poncirus trifoliata L. Raf.*) (Debernardi *et al.*, 2020). *GRF* and *GIF* are transcription factors regulating growth and development of plants, and their ability to enhance the efficiency of transformation has been extended to maize (*Zea mays*), watermelon (*Citrullus lanatus*), and lettuce (*Lactuca spp*). The combination of *GRF-GIF* with *BBM* improved the transformation efficiency of maize seedlings from 26% to 37% (Chen *et al.*, 2022). Furthermore, in watermelon, overexpression of the *GRF-GIF* chimeric gene resulted in higher transformation efficiency than control conditions

109 (Feng *et al.*, 2021). The *GRF-GIF* chimera with mutated miRNA396 improved the regeneration
110 and shooting efficiency in lettuce (Bull *et al.*, 2023).
111 Here we describe a transformation protocol for *C. campestris* that was developed through
112 exploration of several different reporter genes and morphogenic genes. Although *Cuscuta*
113 species have been broadly regarded as recalcitrant to transformation, the technique readily
114 generates transgenic *C. campestris* plants that show normal coiling and haustorium formation,
115 and ultimately produce flowers and seeds. This approach unlocks new possibilities for
116 conducting functional studies on *Cuscuta* and facilitates investigations into understanding of
117 plant-plant interactions.
118

Materials and methods

Cuscuta seed scarification and germination

C. campestris seedlings were attached to 3-week-old beets (Detroit Dark Red, *Beta vulgaris*) and grown in a greenhouse with a temperature of 25°C - 30°C and a day/night length of 16/8 hours. The use of beet as a nursery host for *C. campestris* is a coincidence that has nothing to do with the use of the RUBY marker; beet has a low growth profile, plentiful petioles, and high susceptibility, so it is an excellent host for the parasite. Three months after the inoculation, *Cuscuta* seeds were collected and cleaned. To promote germination, clean seeds were scarified as described previously (Bernal-Galeano *et al.*, 2022). Scarified seeds were rinsed with autoclaved water three times, sterilized with 3% sodium hypochlorite for 15 minutes, washed with autoclaved water five times and incubated at 4°C overnight. For seed germination, 100 *Cuscuta* seeds were placed on a petri dish with a wet Whatman's 3MM paper and incubated at 28°C without light for two days. The petri dish containing *Cuscuta* seedlings was placed to a growth chamber set to 25 °C with 16 hours of light and 8 hours of darkness using Lithonia Lighting Fluorescent Luminaire bulbs (Model: C 2 32 120 GESB) that provided 300-400 lux of illumination and incubated for one day to be 3-day-old seedlings.

Agrobacterium-mediated *Cuscuta* transformation

To develop the *Agrobacterium*-mediated *Cuscuta* transformation protocol, we tested three different conditions including optimization of media growth hormone concentrations, simplified inoculation process with RUBY, and stable generation of *Cuscuta* transgenic lines.

First protocol - *Optimization of media growth hormone concentrations*: A single colony of *A. tumefaciens* EHA105 containing the *35S:GUS-pMAS:GFP* (Supp Figure 1A) was inoculated into 1-2 mL of liquid MGL medium and incubated at 29°C with shaking at 200 rpm for 48 hours. The bacterial culture was then spread on a solid MGL plate and incubated overnight at 29°C. The resulting creamy bacterial culture was used for inoculating the explant (Supp Figure 1B). Three-day-old seedlings (Supp Figure 1C), as described in the seed germination section, were infected with *Agrobacterium* using the streak infection method from the previous protocol (Kanchanamala & Bandaranayake, 2019). The 3-day-old seedling's apical part without meristem was cut from each plant (Supp Figure 1D-E) (Furuhashi *et al.*, 2012) and dipped in the creamy bacteria culture for 3-5 seconds (Supp Figure 1F). The explants were placed on co-cultivation media (CCM) containing 3 mg/L Naphthalene Acetic Acid (NAA) (N0640, Sigma) and 1 mg/L

150 Benzylaminopurine (BAP) (B3274, Sigma) for co-cultivation at 15ºC for 7 days with 16 hours of
151 light and 8 hours of darkness condition (Supp Figure 1G and Supp Table 1). Subsequently, the
152 infected explants (Supp Figure 1G) were transferred to MMS media containing antibiotic
153 cefotaxime (250 mg/L) (C-104-5, GoldBio), cytokinins, and auxins (Supp Figure 1I and Supp
154 Table 1). We tested NAA at concentrations of 0 and 0.5 mg/L, BAP at 5, 7.5, 10, and 25 mg/L,
155 Thidiazuron (TDZ) (P6186, Sigma) at 0.05, 0.1, 0.3, and 0.5 mg/L and MMS media without any
156 growth hormones. We designed a factorial experiment to observe the ideal plant growth hormone
157 combination for better transformation efficiency.

158 Second protocol - *Simplified inoculation process with RUBY*: To simplify the inoculation
159 process, we developed a bulk chopping method that is less precise but quicker than carefully
160 dissecting out the shoot apical region. The laborious dissecting method was termed the "cut"
161 technique, and the more random method was termed the "bulk chop" technique. We compared
162 the transformation efficiencies between the cut and bulk chop methods for preparing *Cuscuta*
163 segments. Using a sterilized surgical blade, a large mass of 3-day-old seedlings from 200 seeds
164 was chopped into small pieces to make around 5mm segments, which greatly facilitated the
165 tissue preparation step and produced a large number of potentially transformable sections at
166 once. Also, instead of a construct with GUS and GFP reporters, we used a construct containing
167 *35S:RUBY* (He *et al.*, 2020). *A. tumefaciens* EHA105 harboring the construct *35S:RUBY* was
168 strecked on a LB plate and incubated at 28 ºC for two days. A single colony was cultured in 5mL
169 liquid media and grown in a shaker at 28 ºC for 16 hours. This culture was subsequently
170 subcultured in 50mL of LB liquid media and incubated for another 16 hours at 28 ºC. When the
171 OD600 reached 1.0 to 1.2, the cells were harvested and resuspended in liquid MMS media
172 without a growth hormone. Infected explants were placed on CCM for 5 days and then
173 transferred to CIM containing Cefotaxime (250 mg/L) and BAP (5 mg/L) (Supp Table 1).
174 Transformed tissues expressing RUBY were counted around a month after inoculation.

175 Third protocol - *Stable generation of Cuscuta transgenic lines*: Three-day-old *Cuscuta*
176 seedlings were bulk-chopped into small pieces as described in the second protocol. The bacteria
177 were prepared following a procedure similar to the second protocol. After cocultivation with *A.*
178 *tumefaciens* EHA105 solutions, *Cuscuta* seedlings were uniformly distributed and incubated on
179 co-cultivation media for five days (Supp Table 2). After the co-cultivation stage, infected
180 seedlings were transferred to Callus Induction Media (CIM) containing 5 mg/L BAP and 250

181 mg/L cefotaxime (Supp Table 2). For the GUS staining assay, calli were harvested 30-35 days
182 after infection. To generate stably transformed *Cuscuta*, calli were incubated on CIM for at least
183 8 weeks, shoot induction media (SIM) for at least 8 weeks, and shoot elongation media (SEM)
184 for 3-4 weeks (Supp Table 2). Media with explants were replaced with new media every two
185 weeks.

186 The co-cultivation, callus induction, shoot induction, and shoot elongation processes for the
187 first, second, and third protocols were conducted under the following conditions: 25 °C with 16
188 hours of light and 8 hours of darkness using Lithonia Lighting Fluorescent Luminaire bulbs
189 (Model: C 2 32 120 GESB), providing 300-400 lux of illumination.

190 **GUS staining and GFP observation**

191 For the GUS staining, *Cuscuta* calli were incubated in X-Gluc solution (G1281C2, GoldBio)
192 for up to 24 hours and then destained in 95 % Ethanol (Park *et al.*, 2022). Images were captured
193 using Leica Thunder imager M205 FA model stereomicroscopy system.

194 Fluorescent signals were detected with both Leica Thunder imager M205 FA model
195 stereomicroscopy system and Leica SP8 spectral confocal microscope. All microscopy for GUS
196 and fluorescence expression was conducted at the Advanced Light Microscopy Core
197 (https://research.missouri.edu/advanced-light-microscopy), University of Missouri. GFP and
198 RFP expression patterns were imaged with the following setting (excitation/emission): GFP at
199 488 nm / 510 nm and RFP at 561 nm / 584nm. RFP was used as a negative control.

200 **Vibratome sectioning and imaging**

201 *Cuscuta* haustoria expressing RUBY or WT *Cuscuta* grown on tomato (*Solanum*
202 *lycopersicum* var. Rutgers) or *Arabidopsis* Col-0 for two weeks were harvested and embedded in
203 5 % Agarose (Park *et al.*, 2022). Tissue sectioning was performed using a Leica series Vibratome
204 3000 Plus. Longitudinal and transverse sections were cut with thickness ranging from 250µm to
205 400µm, depending on the softness of the tissue. Sections were stained by 0.02% toluidine blue
206 (T3260, Sigma) (Pradhan Mitra & Loqué, 2014). For imaging, sections were placed on
207 microscope slides and imaged by Leica M205 FA automated stereo microscope.

208 **Thermal asymmetric interlaced (TAIL)-PCR**

209 To confirm T-DNA insertions in transgenic *Cuscuta*, genomic DNAs of transgenic *Cuscuta*
210 *35S:RUBY* No. #9a and No. #18a were extracted using Cetyltrimethylammonium-bromide
211 (CTAB) (Sigma), and TAIL PCRs were conducted using insertion-specific primers (RB1 and

212 RB2) and arbitrary degenerate primers (AD primers) using primary and secondary PCR
213 conditions (Supp Tables 3 and 4). Specific bands from amplification with AD and RB2 primers
214 were extracted and sequenced. The presence of T-DNA insertions in transgenic RUBY *Cuscuta*
215 plants was verified by aligning the sequencing results with a *Cuscuta campestris* genome
216 sequence (Vogel et al., 2018).

217 **Vector constructions**

218 *35S:GUS-pMAS:GFP* (Supp Figure 1A) was modified by replacing the 35S promoter with
219 the MAS promoter from *pGFPGUSPlus* (Plasmid #64401, Addgene) (He *et al.*, 2020) because
220 *pMAS:GFP* showed stronger expression than *35S:GFP* (Mudalige *et al*., under preparation).

221 *CcGRF* and *CcGIF* were identified from the *C. campestris* genome (Vogel *et al*., 2018) via
222 sequence alignments and phylogenetic trees including wheat homologs (Debernardi *et al*., 2020),
223 performed in the Geneious Prime 2022.2.2 software. The selected *CcGRF* homolog Cc010427
224 and *CcGIF* homolog Cc021394 were cloned and sequenced using gene specific primers (Supp
225 Table 5). The confirmed clones were ligated to make a *CcGRF/CcGIF* fusion via the Golden
226 Gate method using NEB's NEBridge kit and re-cloned into Pcr8GWTOPO vector (Invitrogen).

227 *CcWUS2* was synthesized by Azenta life science (www.azenta.com) and re-cloned into
228 Pcr8GWTOPO vector.

229 *CcWUS2* and *CcGRF/GIF* in entry clone pCR8GWTOPO were incubated with LR clonase
230 and pMDC139 to generate destination vectors with genes of interest (*35S:CcWUS2-GUS* and
231 *35S:CcGRF/CcGIF-GUS*). *35S:GUS-MAS:GFP*, *35S:CcWUS2-GUS*, and *35S:CcGRF/GIF-GUS*
232 were transformed into *A. tumefaciens* EHA105 strain by the freeze-thaw transformation method
233 (Weigel & Glazebrook, 2006).
234

235 **Results**

236 **Test of hormones and media composition for *C. campestris* transformed calli**

237 To establish the transformation protocol for *C. campestris*, we initially tested various
238 concentrations of NAA and cytokinin (BAP/TDZ) in a medium designed for both co-cultivation
239 and callus induction (Supp Table 1) using the first protocol described in the material and method
240 section (Supp Figure 1). A negative control, consisting of the same medium without growth
241 hormones, was also employed. Approximately thirty days after inoculation with *A. tumefaciens*
242 EHA105-*35S:GUS-pMAS:GFP* (Supp Figure 1A), transformation efficiency was assessed by
243 GFP expression using a stereomicroscope (Supp Figure 2A-D). Cells expressing GFP (Supp
244 Figure 2A and 2D) but not RFP (Supp Figure 2B) were counted as transformed tissue (Supp
245 Table 6). Additionally, a confocal microscope revealed that GFP was located in the nucleus and
246 cytoplasm, which is typical GFP localization (white arrows, Supp Figure 2E). The merged image
247 of GFP, RFP, and bright field demonstrated GFP-specific expression in a month-old explant
248 (Supp Figure 2D, 2H, and 2I).

249 Using the first transformation method and a GFP reporter construct, we compared
250 transformation efficiencies between different treatments (Supp Figure 3 and Supp Table 6). The
251 statistical analysis indicated a significantly higher GFP expression in the media containing plant
252 growth regulators compared to that without hormones (Supp Figure 3). *Cuscuta* explants
253 cultivated on CIM media with BAP or TDZ without NAA exhibited significantly higher GFP
254 expression than those on CIM media with NAA or the no hormone media, indicating that the
255 presence of cytokinin hormones had a positive effect while the presence of NAA had a negative
256 impact on efficiency. However, there was no significant difference among treatments with
257 different concentrations of BAP or TDZ. Thus, we concluded that the presence of BAP or TDZ
258 without NAA in the CIM culture media significantly enhanced the *C. campestris* transformation
259 efficiency. For subsequent experiments, we used 5 mg/L BAP to induce *Cuscuta* callus in CIM
260 media.

261 **Comparison of the transformation efficiency of explants prepared with the cut versus the**
262 **bulk chop method using the RUBY reporter**

263 While approximately 50% of *Cuscuta* calli expressed GFP 30 days after *A. tumefaciens*
264 inoculation and cultivated on 5mg/L BAP media (Supp Figure 2), the preparation of individual
265 meristems through the cut method (Supp Figure 1D) is labor-intensive, as it involves the

266 individual handling of each seedling. We tested a simpler bulk chop method that produced a
267 large amount of *Cuscuta* segments for potential transformation. In this comparison, both cut and
268 bulk chop samples were infected with *A. tumefaciens* EHA105-*35S:RUBY* and incubated on
269 CIM for 30 days (Supp Table 1). RUBY encodes enzymes for the synthesis of betalain and is
270 useful for visually monitoring transformation events without staining or special equipment. Calli
271 derived from the cut method exhibited 100% RUBY expression, whereas calli from the bulk
272 chop method displayed relatively lower RUBY expression (65%) (Supp Table 7). Previously we
273 found thatthe shoot apical part of *Cuscuta* generated more callus and transformable tissue than
274 other parts (Mudalige et al., under preparation). Thus, we hypothesize that the bulk chop method
275 had lower RUBY expression than the cut method because the non-transformable tissues
276 including root or shoot tips were included with the transformable tissues incubated on the media.
277 In addition, calli expressing RUBY from the cut method (Figure 1A-C) did not exhibit any
278 phenotypic differences when compared to calli from the bulk chop method (Figure 1D-F). As
279 RUBY has been used as a visual selection marker in other plants (Yu *et al.*, 2023), we decided to
280 employ it as a visual selection marker during the early co-cultivation stage, eliminating the need
281 for a selection reagent.

282 ***Agrobacterium*-mediated *Cuscuta* transformation and regeneration of transgenic plants**

283 To conduct the *Agrobacterium*-mediated *Cuscuta* transformation, three-day-old seedlings
284 from 200 *C. campestris* seeds were chopped and infected with *A. tumefaciens* EHA105-
285 *35S:RUBY* as described in the third protocol, the method section. *Agrobacterium* infected
286 segments were incubated on the co-cultivation media for five days (Figure 2A). Subsequently,
287 100 selected *Cuscuta* segments expressing strong RUBY were divided among two CIM media
288 plates, each containing 50 explants per plate (Figure 2B). Explants were incubated in CIM media
289 for a minimum of 8 weeks before being transferred to shoot induction media (Figure 2C-D).
290 Larger and darker red calli were obtained after another 8 weeks of incubation on the shoot
291 induction media (Figure 2E-F) and then transferred to shoot elongation media when the red calli
292 reached a size of 1 cm (Figure 2 G-H). Calli grown on the shoot elongation media started to
293 produce shoots in two weeks (Figure 2I).

294 During the callus induction stage, the number of visible red spots on *A. tumefaciens*
295 EHA105-*35S:RUBY* infected *Cuscuta* segments were counted on 5, 15, 25, 35, and 45 days after
296 infection to track the transformation efficiency. Since we selected 100 *Cuscuta* segments

297 expressing RUBY from 200 *Cuscuta* seeds to callus induction media after 5-day co-cultivation
298 on each replicate, transformed calli represented 100% on the fifth day of inoculation. The
299 number of transformed calli slowly declined to 93.2%, 86.0%, 76.7 %, and 62.1% on the 15, 25,
300 35, and 45 days after inoculation, respectively (Figure 3A and Supp Table 8).
301 Further declines in the number of stably transformed calli occurred over subsequent growth
302 stages. Percentages of RUBY calli growing on SEM, RUBY calli developing shoots, and RUBY
303 *Cuscuta* coiled on host plants were 16%, 5.3%, and 2.8%, respectively (Figure 3B and Supp
304 Table 9).

305 **Successful parasitism of transgenic RUBY *Cuscuta***

306 Once the RUBY *Cuscuta* shoots reached a size of 3 cm on the shoot elongation media, calli
307 with RUBY *Cuscuta* shoots were moved to magenta boxes containing the shoot elongation
308 media (Figure 4A). To observe the characteristic coiling behavior of *Cuscuta*, a toothpick was
309 inserted into the media to serve as a substitute host. Within a day of introducing the toothpick,
310 RUBY *Cuscuta* coiled (Figure 4B) and produced haustoria (Figure 4C). We also introduced
311 RUBY *Cuscuta* stems to live host plants. Within 24 hours post-inoculation, the RUBY *Cuscuta*
312 stems exhibited coiling and initiated haustoria development on a 1-week-old tomato (Figure 4D).
313 All host plants, both tomatoes (Figure 4E) and *Arabidopsis* (Figure 4F) were successfully
314 parasitized by the RUBY *Cuscuta*. Approximately 2 months after transfer to beet hosts, RUBY
315 *Cuscuta* produced flowers (Figure 4G-H) and seeds (Figure 4I).
316 Seeds from a T0 transgenic *Cuscuta* (*35S:RUBY* No. #10a1) were germinated to analyze
317 RUBY and non-RUBY segregation ratios. Transgenic *Cuscuta 35S:RUBY* No. #11 exhibited
318 similar germination efficiency compared to wild-type *Cuscuta* with RUBY and non-RUBY
319 segregation ratio of 2.33 : 1 ± 0.58 (Supp Table 10). The transgenic seedlings showed distinct
320 betalain pigments throughout their entire tissues (Supp Figure 4). This suggests that the RUBY
321 transgene from T0 transgenic *Cuscuta* is stably inherited by the next generation through
322 *Agrobacterium*-mediated *Cuscuta* transformation.

323 **Event-specific detections of transgenic lines**

324 From 8 attempts of the *Agrobacterium*-mediated *Cuscuta* transformation, 11 transgenic
325 events were generated and successfully coiled on host plants (Supp Table 9). To validate the T-
326 DNA insertions, gDNA was extracted from 2 mature transgenic *Cuscuta* (No. #9a and #18a), and
327 TAIL-PCRs using right border (RB) primers located in the 35S promoter of the *35S:RUBY* were

328 conducted (Figure 5A). After sequencing the amplicons, results revealed that both transgenes
329 lacked the RB sequences (gray box, Figure 5A). Furthermore, the transgene of the first event
330 contained a complete 35S promoter, whereas the transgene from the second event had a
331 truncated 35S promoter. By aligning TAIL-PCR sequences with *C. campestris* genome data, the
332 integration locations of transgenes of *35S:RUBY* No. #9a and *35S:RUBY* No. #18a were located
333 on *C. campestris* Scaffold 32B and *C. campestris* Scaffold 104, respectively (Figure 5B and
334 Supp Figure 5). Thus, this result indicates that the transgenic events were independent transgenic
335 plants.

336 **RUBY pigments as markers of haustorial presence and activity in host stems**

337 One advantage of having a transgenic parasite is the opportunity to explore haustorial
338 development and function. Given that RUBY is an excellent visual marker, transgenic *C.*
339 *campestris* was studied in interactions with tomato seedlings and *Arabidopsis* floral stems
340 (Figure 6 and Supp Figure 6). The negative control tissues from tomato and *Arabidopsis* did not
341 exhibit any pigment accumulation inside stems (Supp Figure 6A - 6B). WT *C. campestris* is
342 shown coiled around a tomato stem with the haustoria invading the host tissue to establish
343 vascular connections (Figure 6A - 6B). Cells of the haustoria are easily identifiable near their
344 base (Figure 6B asterisk) but are difficult to distinguish from host cells near the haustorial tip.
345 When RUBY *Cuscuta* coiled on the host stem but prior to penetration, the red pigment was not
346 detected in host stems or vascular bundles (Figure 6C - 6D). Invasive growth of the haustorium
347 is clear in the host stem during the early haustorium development (Figure 6E – 6F). Mature
348 haustoria are visible within the host root (Figure 6G -6H). Interestingly, we observed diffuse
349 RUBY pigments beyond the area where haustoria cells were clearly detected (Figure 6G and
350 white circles of 6H). Some searching hyphae cells were distinctly visible (black arrows, Figure
351 6H), and stand in contrast to the more diffuse pigment. The diffuse pattern of RUBY pigment
352 was also observed when RUBY *Cuscuta* was grown on *Arabidopsis* Col-0 plants. After staining
353 tissues with toluidine blue, we found that RUBY pigments were mainly detected on cortex and
354 phloem of host *Arabidopsis* stem (Figures 6I-6K). RUBY was even detected in the outside
355 surface of the host stem near haustoria (white arrows of Supp Figures 6D and 6E) and regions
356 away from *Cuscuta* haustoria (white circles of Figures 6I and 6L and white arrows of Supp
357 Figures 6F and 6G). However, *Arabidopsis* with WT *Cuscuta* did not exhibit any pigment
358 accumulation on the surface (Supp Figure 6C) or inside the stem (Supp Figure 6F). The

359 mechanism of pigment spread, whether it represents movement of the pigment itself or some
360 combination of RUBY mRNA/protein, will be a point for future research, but illustrates the
361 potential for using transgenic *Cuscuta* for investigating parasite-host communication.

362 **Enhanced transformation efficiency using *CcGRF/GIF Cuscuta***

363 Morphogenic genes have been reported to enhance plant transformation efficiency (Lowe *et*
364 *al.*, 2016; Chen *et al.*, 2022), so we tested whether *C. campestris WUS2* or *C. campestris*
365 *GRF/GIF* can promote transformation efficiency. Instead of the RUBY reporter, we decided to
366 use the GUS reporter gene to eliminate potential tyrosine deficiency phenotype caused by the
367 RUBY reporter (Lee *et al.*, 2023). Three-day-old *C. campestris* seedlings (Figure 7A) were bulk
368 chopped and infected by EHA105 with *GUS*, *CcWUS2-GUS,* and *CcGRF/GIF-GUS* (Figure 7B).
369 After the co-cultivation, 50 infected meristem-containing-segments were placed on CIM media
370 (Figure 7C). Around 35 days of incubation on CIM, *Cuscuta* segments infected by EHA105
371 with *GUS*, *CcWUS2-GUS,* and *CcGRF/GIF-GUS* were harvested and stained (Figure 7D-F).
372 Segments expressing GUS were quantified and classified by sizes of the GUS expressing sectors,
373 such as no GUS, less than 0.2 mm GUS, between 0.2 to 2 mm GUS, and larger than 2 mm GUS,
374 aiming to distinguish the extent of GUS expression in a segment (Supp figure 7).

375 In terms of presence and absence of GUS expression, the transformation efficiencies using
376 *GUS*, *CcWUS2-GUS,* and *CcGRF/GIF-GUS* were 78.8%, 51.7%, and 74.8%, respectively
377 (Figure 8A). Notably, the transformation efficiency associated with *CcWUS2-GUS* was
378 significantly lower than *GUS* or *CcGRF/GIF-GUS.* In contrast, there was no significant
379 difference in transformation efficiency between GUS and *CcGRF/GIF-GUS*. Data from
380 categorized segments indicated that *Cuscuta* segments transformed with *GUS* alone showed a
381 significantly higher proportion of expressing tissues in the below 0.2 mm category compared to
382 those transformed with morphogenic gene fusions *CcWUS2-GUS* and *CcGRF/GIF-GUS* (Figure
383 8B). *Cuscuta* with *CcGRF/GIF-GUS* had a significantly higher percentage in the over 2mm
384 group than *GUS* only. These findings suggest that *GUS* alone and *CcGRF/GIF-GUS* had similar
385 levels of transformation efficiency based on the presence or absence of GUS expression.
386 However, *CcGRF/GIF-GUS* significantly enhanced regeneration efficiency during the callus
387 induction stage, leading to more significant GUS expression compared to *GUS* alone.
388

Discussion

The lack of a protocol for transformation and regeneration of *Cuscuta* has hindered progress in studying parasite gene functions and the mechanisms of *Cuscuta*-host interactions. Despite previous studies demonstrating transformation of *Cuscuta* tissues (Borsics *et al.*, 2002; Švubová & Blehová, 2013; Lachner *et al.*, 2020), none have succeeded in regenerating stably transformed *Cuscuta* plants that can be used to study the full range of parasite biology. Here we describe a method for the relatively fast and efficient stable transformation of *C. campestris* plants that behave as normal parasites, producing haustoria, flowers, and seeds (Figure 4). The process hinges on *A. tumefaciens*-mediated transformation with appropriate media for inducing callus and shoots. We estimate that the process took a minimum of 5 months and resulted in a rate of 2.7% recovery of transformed plants from 100 explants expressing RUBY selected during the CIM step. While this transformation efficiency may not be high compared to easily transformable plants like tobacco, it stands out as remarkably successful for a transformation recalcitrant non-model species.

An important innovation in the transformation process was the use of the recently developed RUBY reporter (He *et al.*, 2020). RUBY encodes enzymes for synthesizing betalain from tyrosine and is useful for visually monitoring transformation events without using fluorescence microscopy or a chemical selection process. However, recent studies reported that RUBY may cause low regeneration efficiency and poor fertility during seed development due to the lack of the essential amino acid tyrosine. For example, maize expressing a strong RUBY reporter had growth retardation (Lee *et al.*, 2023). While we are mindful that the RUBY reporter could be detrimental to *Cuscuta*, evidence to date suggests that transgenic RUBY *Cuscuta* shows normal, though somewhat slower, growth compared to non-transgenic plants. But importantly, the vivid RUBY reporter proved to be an invaluable asset in the development of the protocol. Its strong visible color and non-reliance on toxic selection reagents make it difficult to replace with other selectable markers..

The use of morphogenic genes appears to contribute positively to the *Cuscuta* transformation protocol. We observed an enhancement in transformation efficiency with *Cuscuta GRF-GIF*, a phenomenon similar to previously reported findings in wheat and citrus transformation (Debernardi *et al.*, 2020). In *Agrobacterium*-mediated *Cuscuta* transformation, *CcGRF-GIF* showed minimal impact on the overall presence/absence ratios of GUS transformation efficiency

420 (Figure 8A). However, the number of GUS segments larger than 2mm was significantly
421 increased in *CcGRF-GIF-GUS* infected *Cuscuta* compared to *Cuscuta* segments that had been
422 transformed with *GUS* alone (Figure 8B). This suggests that *CcGRF-GIF* may not significantly
423 influence *Agrobacterium*-mediated transformation but could enhance the regeneration of
424 transformed tissue, as previously reported (Debernardi *et al.*, 2020). Further investigation is
425 needed regarding the utilization of *CcGRF-GIF* with *Cuscuta* transformation. In contrast, using
426 *CcWUS-GUS* in transformations led to lower presence/absence ratios of GUS transformation
427 efficiency than *GUS* alone or *CcGRF-GIF-GUS* (Figure 8A). We hypothesize that, similar to
428 previous studies, the constitutive *CcWUS2* expression by the 35S promoter may interfere with
429 the *Cuscuta* development genes, resulting in the decreased transformation efficiency (Rashid *et*
430 *al.*, 2007; Lowe *et al.*, 2016; Hoerster *et al.*, 2020; Kadri *et al.*, 2021).
431 Observing the interaction of RUBY expressing *Cuscuta* and its hosts suggests that the RUBY
432 reporter system serves not only as a selection marker for transformation, but also as an indicator
433 of events during parasitism at the molecular level. We were able to monitor the invasion progress
434 of the haustorium and observe what appears to be movement of RUBY pigment from the
435 transformed parasite into host cells in the area around developed *Cuscuta* searching hyphae
436 (Figure 6H, K). We do not think this is an artefact of sectioning as the RUBY diffusion was not
437 observed during the early invasion stage (asterisk, Figure 6G). This finding is intriguing given
438 the ability of *Cuscuta* to exchange not only small molecules, but also mobile mRNAs, small
439 RNAs and proteins with its host plants (Kim *et al.*, 2014; Park *et al.*, 2022)(Shahid *et al.*, 2018).
440 Unfortunately, the current data do not allow confident identification of the mechanism of
441 pigment movement. Potential explanations for the movement could include: 1) translation of
442 mobile RNA, wherein mRNAs of betalain synthesis enzymes move from *Cuscuta* to the host
443 stem and are translated near the haustoria; 2) mobile proteins from *Cuscuta* to host, involving the
444 export of three betalain synthesis enzymes from *Cuscuta* that produced betalain in the host stem;
445 or 3) the movement of betalain pigment itself from *Cuscuta* to the host. The last of these options
446 would seem to be the simplest, but betalain is normally sequestered in vacuoles and is not
447 translocated (Chen *et al.*, 2017), and *C. campestris* growing on beet does not take up pigment
448 from its host (Park and Westwood, personal observations). Fortunately, we now have the tools to
449 validate these hypotheses. It would be interesting to generate transgenic *Cuscuta* expressing a
450 fluorescence reporter gene fused with endoplasmic reticulum (ER) targeting peptide, such as ER-

YFP (Sager *et al.*, 2020), which produces a non-mobile product that would provide a definitive marker of parasite cells. Further research is needed, but regardless of the details, the ability to generate transgenic *Cuscuta* as described here will enable many more experiments, and much greater understanding, of *Cuscuta* biology.

Acknowledgement

This work was supported by the USDA-AFRI- 2023-67013-39896 to SP and JW, CAFNR-JOY, University of Missouri to SP, Research Council, University of Missouri to SP and NSF award IOS-1645027 to JW. We thank Duy Trinh who made the *CcGRF-GIF* construction. Grammarly generated responses to the following AI prompts: Prompts created by Grammarly- "Improve it".

Conflicting interests

All authors declare that they have no conflicting interests**.**

Author contributions

SP, HL, and JW conceived the ideas and designed methodology. SA, AM, VB, HG, and SP conducted lab-work and analyzed the data. SA, AM, SP, and JW led the writing of the manuscript. All authors contributed critically to the drafts and gave final approval for publication.

Data availability

The datasets used and/or analyzed during the current study are available from the corresponding author upon request.

References

Bandaranayake PCG, Yoder JI. 2018. Factors affecting the efficiency of Rhizobium rhizogenes root transformation of the root parasitic plant Triphysaria versicolor and its host Arabidopsis thaliana. *Plant Methods* **14**: 61.

Bernal-Galeano V, Beard K, Westwood JH. 2022. An artificial host system enables the obligate parasite Cuscuta campestris to grow and reproduce in vitro. *Plant Physiology* **189**(2): 687-702.

Borsics T, Mihálka V, Oreifig AS, Bárány I, Lados M, Nagy I, Jenes B, Toldi O. 2002. Methods for genetic transformation of the parasitic weed dodder (*Cuscuta trifolii* Bab. et Gibs) and for PCR-based detection of early transformation events. *Plant Science* **162**(2): 193-199.

Bull T, Debernardi J, Reeves M, Hill T, Bertier L, Van Deynze A, Michelmore R. 2023. GRF–GIF chimeric proteins enhance in vitro regeneration and Agrobacterium-mediated transformation efficiencies of lettuce (Lactuca spp.). *Plant Cell Reports* **42**(3): 629-643.

Chen N, Yu Z-H, Xiao X-G. 2017. Cytosolic and Nuclear Co-localization of Betalain Biosynthetic Enzymes in Tobacco Suggests that Betalains Are Synthesized in the Cytoplasm and/or Nucleus of Betalainic Plant Cells. *Frontiers in Plant Science* **8**.

Chen Z, Debernardi JM, Dubcovsky J, Gallavotti A. 2022. Recent advances in crop transformation technologies. *Nature Plants* **8**(12): 1343-1351.

Cudney DW, Orloff SB, Reints JS. 1992. An Integrated Weed Management Procedure for the Control of Dodder (Cuscuta indecora) in Alfalfa (Medicago sativa). *Weed Technology* **6**(3): 603-606.

Dawson JH, Musselman LJ, Wolswinkel P, Dörr I. 1994. Biology and control of Cuscuta. *Reviews of Weed Science* **6**: 265-317.

Debernardi JM, Tricoli DM, Ercoli MF, Hayta S, Ronald P, Palatnik JF, Dubcovsky J. 2020. A GRF–GIF chimeric protein improves the regeneration efficiency of transgenic plants. *Nature Biotechnology* **38**(11): 1274-1279.

Dechassa N, Regassa B. 2021. Current Status, Economic importance and Management of Dodders (Cuscuta Spp) of Important Crops.

Feng Q, Xiao L, He Y, Liu M, Wang J, Tian S, Zhang X, Yuan L. 2021. Highly efficient, genotype-independent transformation and gene editing in watermelon (Citrullus lanatus) using a chimeric ClGRF4-GIF1 gene. *J Integr Plant Biol* **63**(12): 2038-2042.

Fernández-Aparicio M, Rubiales D, Bandaranayake PC, Yoder JI, Westwood JH. 2011. Transformation and regeneration of the holoparasitic plant Phelipanche aegyptiaca. *Plant Methods* **7**(1): 36.

Furuhashi T, Fragner L, Furuhashi K, Valledor L, Sun X, Weckwerth W. 2012. Metabolite changes with induction of Cuscuta haustorium and translocation from host plants. *Journal of Plant Interactions* **7**(1): 84-93.

Galloway AF, Knox P, Krause K. 2020. Sticky mucilages and exudates of plants: putative microenvironmental design elements with biotechnological value. *New Phytologist* **225**(4): 1461-1469.

Goldwasser Y, Sazo MRM, Lanini WT. 2012. Control of Field Dodder (Cuscuta campestris) Parasitizing Tomato with ALS-Inhibiting Herbicides. *Weed Technology* **26**(4): 740-746.

He Y, Zhang T, Sun H, Zhan H, Zhao Y. 2020. A reporter for noninvasively monitoring gene expression and plant transformation. *Horticulture Research* **7**(1): 152-152.

Hegenauer V, Fürst U, Kaiser B, Smoker M, Zipfel C, Felix G, Stahl M, Albert M. 2016. Detection of the plant parasite Cuscuta reflexa by a tomato cell surface receptor. *Science* **353**(6298): 478-481.

Hegenauer V, Slaby P, Körner M, Bruckmüller J-A, Burggraf R, Albert I, Kaiser B, Löffelhardt B, Droste-Borel I, Sklenar J. 2020. The tomato receptor CuRe1 senses a cell wall protein to identify Cuscuta as a pathogen. *Nature communications* **11**(1): 5299.

Hoerster G, Wang N, Ryan L, Wu E, Anand A, McBride K, Lowe K, Jones T, Gordon-Kamm B. 2020. Use of non-integrating Zm-Wus2 vectors to enhance maize transformation: non-integrating

524 WUS2 enhances transformation. *In Vitro Cellular & Developmental Biology-Plant* **56**(3): 265-
525 279.
526 **Ishida JK, Yoshida S, Ito M, Namba S, Shirasu K. 2011.** Agrobacterium rhizogenes-Mediated
527 Transformation of the Parasitic Plant Phtheirospermum japonicum. *PLoS ONE* **6**(10): e25802.
528 **Johnsen HR, Striberny B, Olsen S, Vidal-Melgosa S, Fangel JU, Willats WGT, Rose JKC, Krause**
529 **K. 2015.** Cell wall composition profiling of parasitic giant dodder (Cuscuta reflexa) and its hosts:
530 a priori differences and induced changes. *New Phytologist* **207**(3): 805-816.
531 **Kadri A, Grenier De March G, Guerineau F, Cosson V, Ratet P. 2021.** WUSCHEL Overexpression
532 Promotes Callogenesis and Somatic Embryogenesis in Medicago truncatula Gaertn. *Plants*
533 *(Basel)* **10**(4).
534 **Kaiser B, Vogg G, Fürst UB, Albert M. 2015.** Parasitic plants of the genus Cuscuta and their interaction
535 with susceptible and resistant host plants. *Frontiers in Plant Science* **6**.
536 **Kanchanamala R, Bandaranayake P. 2019.** An efficient and rapid Rhizobium rhizogenes root
537 transformation protocol for Lemna minor. *Plant Biotechnology Reports* **13**(6): 625-633.
538 **Kim G, LeBlanc ML, Wafula EK, dePamphilis CW, Westwood JH. 2014.** Genomic-scale exchange of
539 mRNA between a parasitic plant and its hosts. *Science* **345**(6198): 808-811.
540 **Lachner LA-M, Galstyan L, Krause K. 2020.** A highly efficient protocol for transforming Cuscuta
541 reflexa based on artificially induced infection sites. *Plant Direct* **4**(8): e00254.
542 **Lanini W, Kogan M. 2005.** Biology and management of Cuscuta in crops. *International Journal of*
543 *Agriculture and Natural Resources* **32**(3): 127-141.
544 **Lee K, Kang M, Ji Q, Grosic S, Wang K. 2023.** New T-DNA binary vectors with NptII selection and
545 RUBY reporter for efficient maize transformation and targeted mutagenesis. *Plant Physiology*
546 **192**(4): 2598-2603.
547 **Lee K, Wang K. 2023.** Strategies for genotype-flexible plant transformation. *Current Opinion in*
548 *Biotechnology* **79**: 102848.
549 **Liu N, Shen G, Xu Y, Liu H, Zhang J, Li S, Li J, Zhang C, Qi J, Wang L, et al. 2020.** Extensive
550 Inter-plant Protein Transfer between Cuscuta Parasites and Their Host Plants. *Mol Plant* **13**(4):
551 573-585.
552 **Lowe K, Wu E, Wang N, Hoerster G, Hastings C, Cho MJ, Scelonge C, Lenderts B, Chamberlin M,**
553 **Cushatt J, et al. 2016.** Morphogenic Regulators Baby boom and Wuschel Improve Monocot
554 Transformation. *Plant Cell* **28**(9): 1998-2015.
555 **Nagar R, Singh M, Sanwal GG. 1984.** Cell Wall Degrading Enzymes in Cuscuta reflexa and Its Hosts.
556 *Journal of Experimental Botany* **35**(8): 1104-1112.
557 **Park SY, Shimizu K, Brown J, Aoki K, Westwood JH. 2022.** Mobile Host mRNAs Are Translated to
558 Protein in the Associated Parasitic Plant Cuscuta campestris. *Plants (Basel)* **11**(1).
559 **Pradhan Mitra P, Loqué D. 2014.** Histochemical staining of Arabidopsis thaliana secondary cell wall
560 elements. *J Vis Exp*(87).
561 **Rashid SZ, Yamaji N, Kyo M. 2007.** Shoot formation from root tip region: a developmental alteration
562 by WUS in transgenic tobacco. *Plant Cell Reports* **26**(9): 1449-1455.
563 **Runyon JB, Mescher MC, De Moraes CM. 2006.** Volatile chemical cues guide host location and host
564 selection by parasitic plants. *Science* **313**(5795): 1964-1967.
565 **Sager R, Wang X, Hill K, Yoo B-C, Caplan J, Nedo A, Tran T, Bennett MJ, Lee J-Y. 2020.** Auxin-
566 dependent control of a plasmodesmal regulator creates a negative feedback loop modulating
567 lateral root emergence. *Nature Communications* **11**(1): 364.
568 **Shahid S, Kim G, Johnson NR, Wafula E, Wang F, Coruh C, Bernal-Galeano V, Phifer T,**
569 **dePamphilis CW, Westwood JH, et al. 2018.** MicroRNAs from the parasitic plant Cuscuta
570 campestris target host messenger RNAs. *Nature* **553**: 82.
571 **Srivastava S, Dwivedi UN. 2001.** Plant regeneration from callus of Cuscuta reflexa–an angiospermic
572 parasite–and modulation of catalase and peroxidase activity by salicylic acid and naphthalene
573 acetic acid. *Plant Physiology and Biochemistry* **39**(6): 529-538.

Švubová R, Blehová A. 2013. Stable transformation and actin visualization in callus cultures of dodder (Cuscuta europaea). *Biologia* **68**(4): 633-640.

Tomilov A, Tomilova N, Yoder JI. 2007. Agrobacterium tumefaciens and Agrobacterium rhizogenes transformed roots of the parasitic plant Triphysaria versicolor retain parasitic competence. *Planta* **225**(5): 1059-1071.

Vaughn KC. 2002. Attachment of the parasitic weed dodder to the host. *Protoplasma* **219**(3): 227-237.

Weigel D, Glazebrook J. 2006. Transformation of agrobacterium using the freeze-thaw method. *CSH Protoc* **2006**(7).

Yu J, Deng S, Huang H, Mo J, Xu Z-F, Wang Y. 2023. Exploring the Potential Applications of the Noninvasive Reporter Gene RUBY in Plant Genetic Transformation. *Forests* **14**(3): 637.

Zuo J, Niu Q-W, Frugis G, Chua N-H. 2002. The WUSCHEL gene promotes vegetative-to-embryonic transition in Arabidopsis. *The Plant Journal* **30**(3): 349-359.

587

588 **Figure 1.** RUBY expression in explants. RUBY expression in cut explants (A, B, C) and bulk chopped
589 explants (D, E, F) approximately 30 days after inoculation.
590

591 **Figure 2**. Process of *Agrobacterium*-mediated *Cuscuta* transformation using *A. tumefacient* EHA105
592 containing *35S:RUBY*. *Cuscuta* seedlings were infected by EHA105-*35S:RUBY* and incubated on CCM
593 for 5 days (A). *Cuscuta* segments expressing RUBY were transferred on CIM from CCM (B). One-
594 month-old RUBY calli and were grown on CIM (C-D) and SIM (E-F). Calli expressing RUBY were
595 selected and transferred to SEM (G-H) and produced shoots (I). (D), (F), and (H) are zoomed images of
596 (C), (E), and (G), respectively.
597

598 **Figure 3**. *C. campestris* transformation efficiency with the RUBY reporter gene. (A) Transformation rate
599 on various days following inoculation. Sixteen independent replicates were performed. (B) The
600 percentage of RUBY calli growing on SEM, RUBY calli producing shoots, and RUBY *Cuscuta* coiled on
601 a live host was quantified. Eight independent replicates were performed. Data are presented as the mean ±
602 standard deviation. Each replicate had 100 explants from 200 *C. campestris* seeds and split into two CIM
603 plates, each containing 50 explants per plate.
604

605 **Figure 4**. Transgenic RUBY *Cuscuta* attaching to non-living and living hosts. A shoot from transgenic
606 callus (A) coiled on a toothpick (B-C). (C) Zoomed-in image of the black box in (B) showing haustoria
607 formation. RUBY *Cuscuta* coiled on (D) and parasitizing (E) the stem of a 2-week-old tomato. (F) RUBY
608 *Cuscuta* was successfully grown on *Arabidopsis*. Transgenic RUBY *Cuscuta* produced flowers on beets
609 (G-H) and seeds (I).
610

611 **Figure 5.** Alignment of sequences from TAIL PCRs and the *35S:RUBY* construct. (A) Diagram of 35S
612 promoter and RUBY near RB region in *35S:RUBY*. Red arrow, yellow arrow, and gray box are RUBY,
613 35S promoter, and right border, respectively. Black arrows (RB1 and RB2) are primers used for the TAIL
614 PCRs. (B) Schematic designs of T-DNA sequences and insertion points into the *C. campestris* genome.
615 Yellow boxes indicate 35S promoter of *35S:RUBY* and white boxes are *C. campestris* genome sequences.
616

617 **Figure 6.** Cross sections of *Cuscuta* haustoria on tomato or *Arabidopsis* stems. Haustoria of WT *C.*
618 *campestris* successfully penetrated tomato stems and established a connection with the host vascular
619 bundle (A-B). RUBY *Cuscuta* coiling around a host tomato stem but failing to penetrate (C-D). RUBY
620 *Cuscuta* successfully attaching to tomato is shown at early (E-F) and mature (G-H) haustoria development

621 stages. (B, D, F, and H): Zoomed-in images of the white box region of corresponding images in (A, C, E,
622 and G). RUBY *Cuscuta* penetrated and developed haustoria on *Arabidopsis* Col-0 stem (I). Images of the
623 white box in (I) before staining (J) and after toluidine staining (K). Vertical section of *Cuscuta*
624 haustorium on *Arabidopsis* Col-0 (L). Asterisks (*), white circles, and black arrows indicate the presence
625 of *Cuscuta* haustorium, area of diffused RUBY pigment, and searching hyphae, respectively. xy, xylem;
626 ixf, xylem fibres; ph, phloem; cor, cortex.
627
628 **Figure 7**. *Agrobacterium*-mediated *Cuscuta* transformation using chopped seedlings. Three-day-old
629 seedlings (A) were chopped (B) and inoculated with *Agrobacterium tumefaciens* strain EHA105
630 harboring *35S:GUS-pMAS:GFP.* (C) Infected segments were incubated on cocultivation media. (D-F)
631 Approximately 35 days after inoculation, segments infected by *35S:GUS-pMAS:GFP, 35S:CcWUS2-GUS*
632 and *35S: CcGRF-CcGIF-GUS* were stained with X-gluc solution.
633
634 **Figure 8.** Effect of *CcWUS2* and *CcGRF/GIF* on *Agrobacterium*-mediated *Cuscuta* transformation. (A)
635 The transformation efficiencies of *GUS* (blue bar), *CcWUS2-GUS* (purple bar), and *CcGRF/GIF-GUS*
636 (pink bar) were compared. (B) GUS expressions were classified into four groups according to the size of
637 GUS expression. Thirty independent replicates were performed. Data are presented as the mean ±
638 standard deviation.
639
640 **Supplementary Figure S1.** Process of *Agrobacterium*-mediated *Cuscuta* transformation with the first
641 protocol. The vector map of *35S:GUS-pMAS:GFP* used for the transformation (A). Solid creamy bacteria
642 culture (B) and three days old *Cuscuta* seedlings (C) and were prepared on the day of inoculation. To
643 obtain a shoot apical part (D), the shoot meristem and middle part were excised using scissors (E). The
644 excised shoot apical part was then immersed in the creamy culture of *A. tumefaciens* EHA105-*35S:GUS-*
645 *pMAS:GFP* (F). Explants were placed on the MMS media with 3mg/L NAA and 5mg/L BAP for co-
646 cultivation (G). An excessive *Agrobacteria* were cultivated from infected tissue seven days after
647 inoculation on the co-cultivation media (H). Explants were incubated on MMS with different Auxin and
648 Cytokinin concentrations (I).
649
650 **Supplementary Figure S2.** GFP, RFP, and bright field images were captured from approximately 1-
651 month-old explants using a stereomicroscope and a confocal microscope. Leica Thunder imager model
652 organism stereomicroscope system detected GFP (A), RFP (B), and bright field (C) images and then
653 merged these three images (D). Leica SP8 spectral confocal microscope detected GFP (E), RFP (F), and
654 bright field (G) and then merged GFP and RFP (H) and GFP, RFP, and bright field images (I).

655

656 **Supplementary Figure S3.** Effect of cytokinins and auxin on GFP positive calli formation after
657 inoculation with *Agrobacterium tumefaciens* EHA105 containing *35S:GUS-pMAS:GFP*. Different types
658 and concentrations of cytokinins (BAP and TDZ) and auxin (NAA) were tested. Six independent
659 biological replicates were performed. Data are presented as the mean ± standard deviation. Groups with
660 different letters vary significantly (two-way ANOVA-Tukey test, P,0.05).

661

662 **Supplementary Figure S4.** Phenotype of T1 transgenic *Cuscuta 35S:RUBY* No. #11. Three-day-old
663 seedlings of wild-type *C. campestris* (A) and 3-day-old T1 transgenic *Cuscuta 35S:RUBY* No. #11 (B).
664 Scarified WT and transgenic seeds were incubated at 4°C overnight, followed by two days in a
665 28°C incubator without light, and then one day under long-day dark/light conditions before being
666 imaged.

667

668 **Supplementary Figure S5.** Results of TAIL-PCRs to confirm genomic integration. Sequences are details
669 of the diagram in Figure 5B. The *35S:RUBY* vector sequences (yellow highlights) are linked to *C.*
670 *campestris* genome scaffolds 32B and 104.

671

672 **Supplementary Figure S6.** Images from sectioned tomato and *Arabidopsis* stems with WT *Cuscuta* or
673 RUBY *Cuscuta*. Rutgers tomato (A) and *Arabidopsis* Col-0 (B) without *Cuscuta* were sectioned and
674 stained by toluidine blue. WT *Cuscuta* growing on *Arabidopsis* Col-0 (C) and RUBY *Cuscuta* growing
675 on *Arabidopsis* Col-0 (D and E) were vertically sectioned (F-H), respectively. White arrows indicate the
676 RUBY pigment on *Arabidopsis* stems.

677

678 **Supplementary Figure S7.** Various sizes of GUS expression sectors in transformed tissues. Following
679 the GUS staining assay, the segments were classified into four groups: No GUS (A-C), less than 0.2 mm
680 GUS (D-F), between 0.2 to 2 mm GUS (G-I), and larger than 2 mm GUS (J-L). The bars represent a scale
681 of 500 μm.

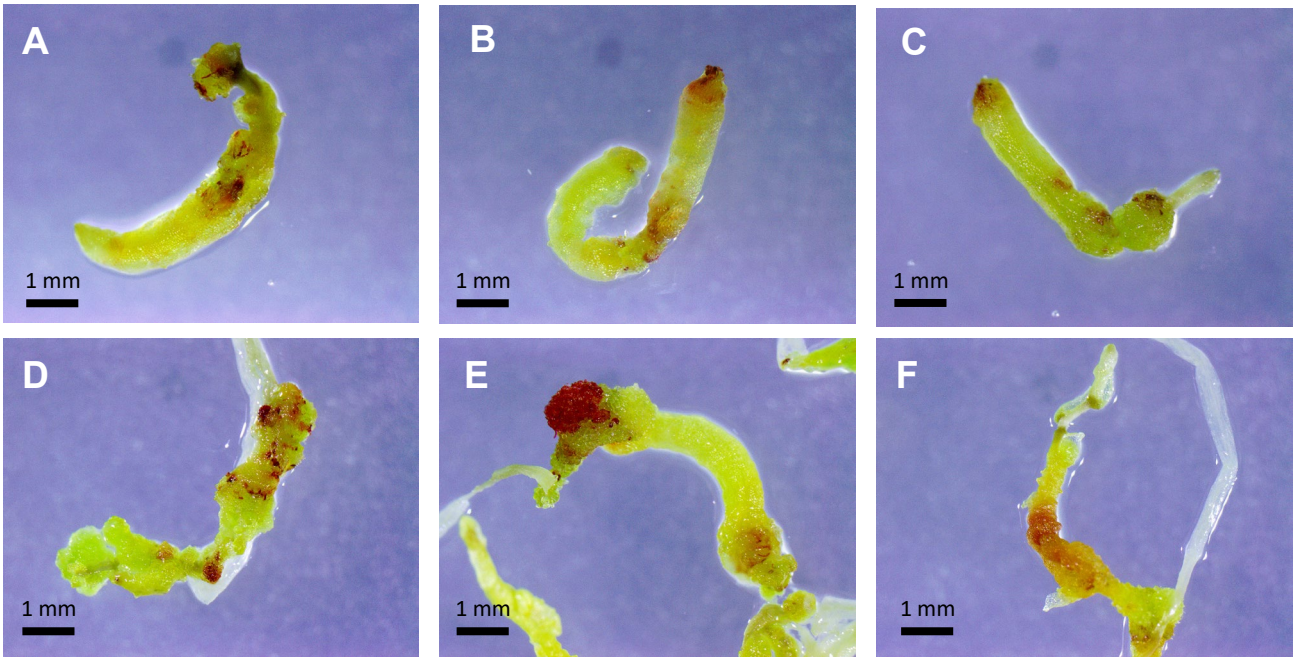

Figure 1

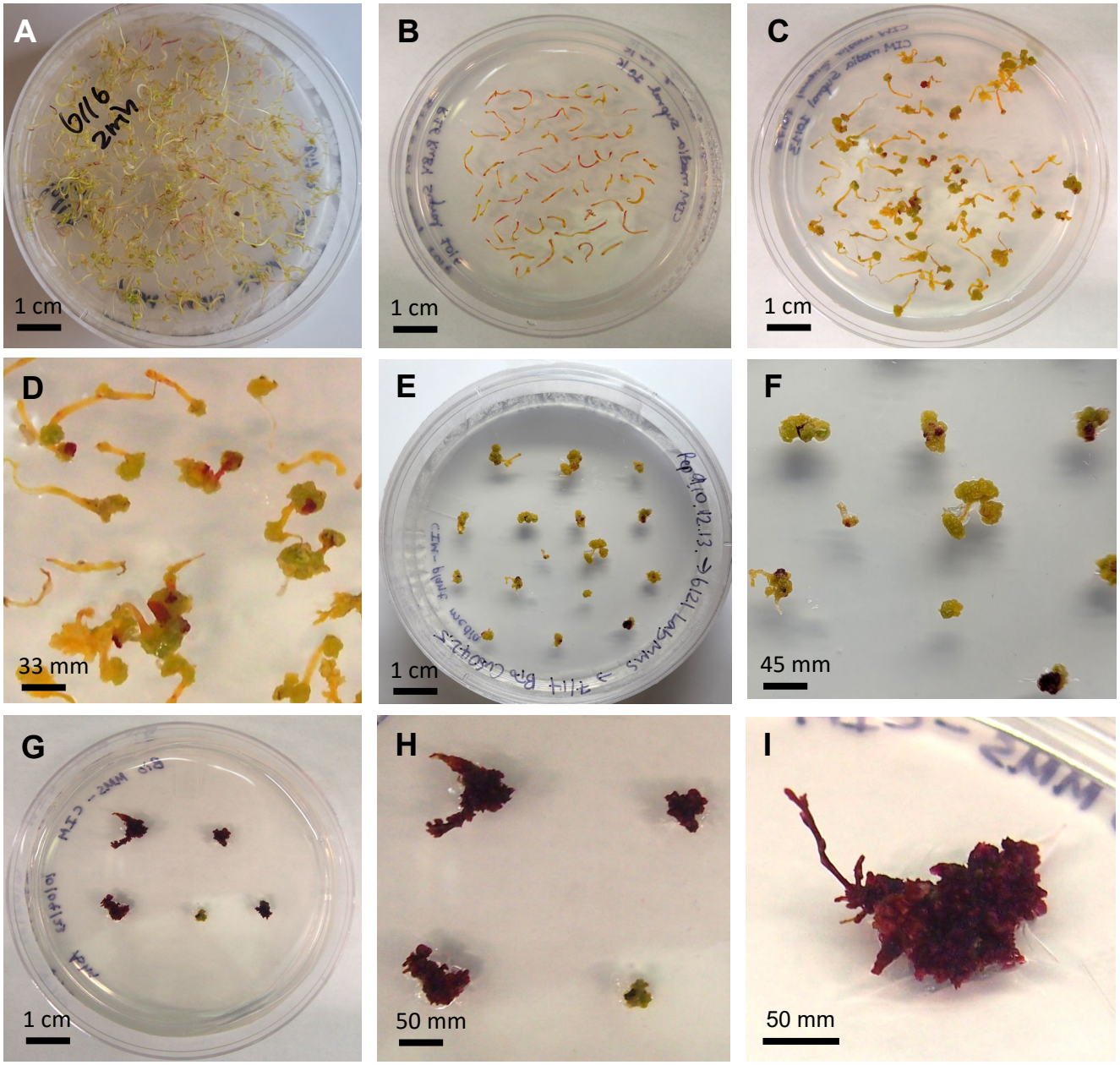

Figure 2

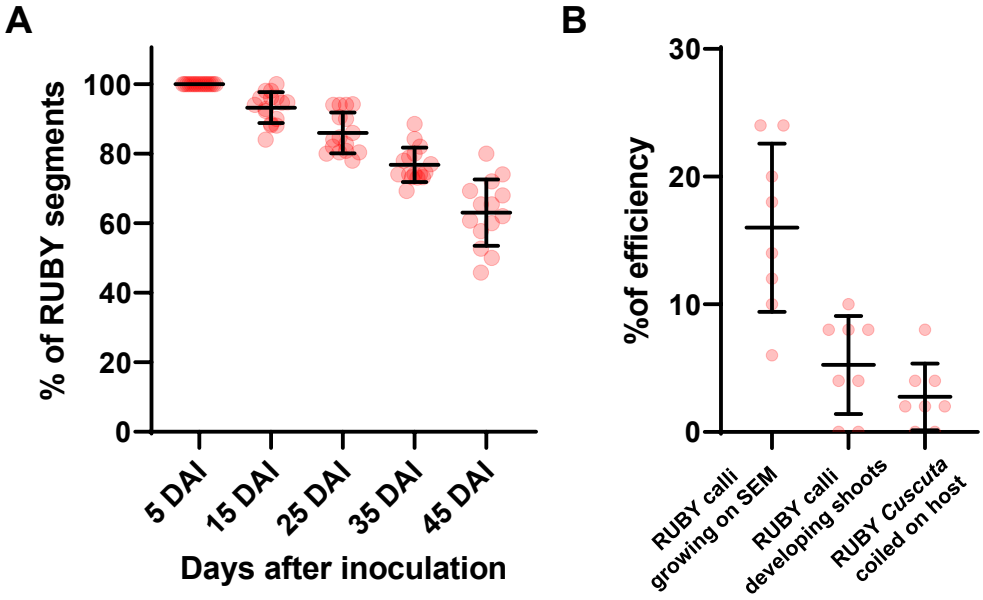
A
% of RUBY segments
100
80
60
40
20
0
5 DAI
15 DAI
25 DAI
35 DAI
45 DAI
Days after inoculation
B
%of efficiency
30
20
10
0
RUBY calli growing on SEM
RUBY calli developing shoots
RUBY Cuscuta coiled on host

Figure 3

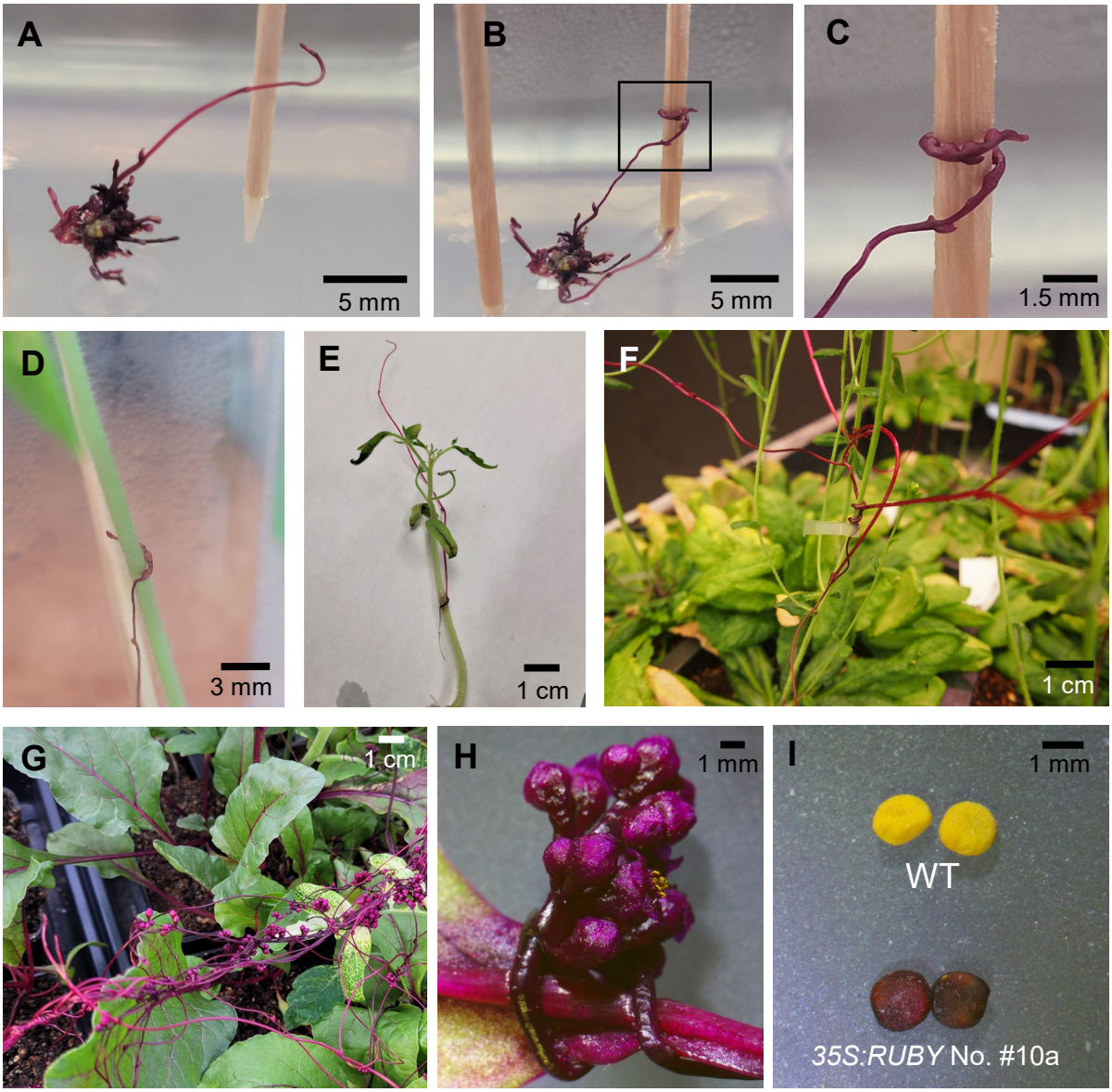
A
5 mm
B
5 mm
C
1.5 mm
D
3 mm
E
1 cm
F
1 cm
G
1 cm
H
1 mm
I
1 mm
WT
35S:RUBY No. #10a

Figure 4

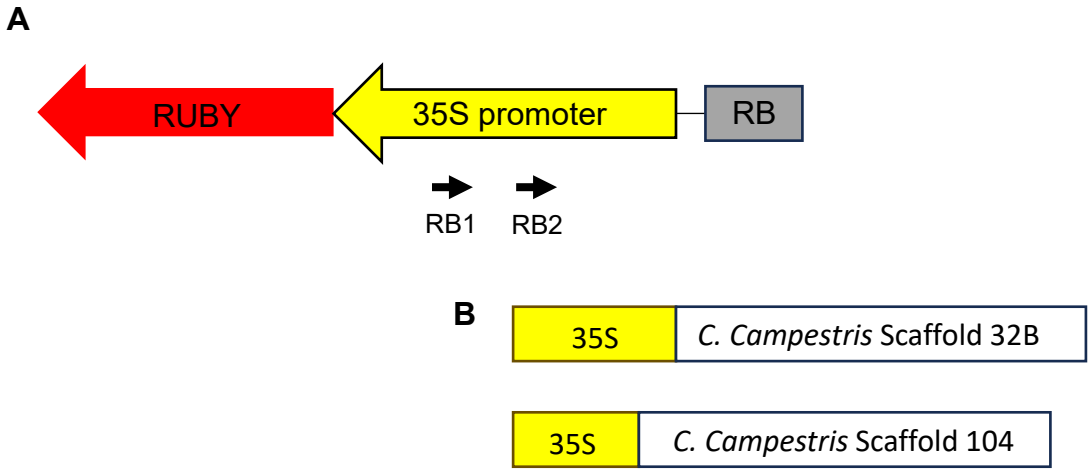
A
RUBY
35S promoter
RB
RB1
RB2
B
35S
C. Campestris Scaffold 32B
35S
C. Campestris Scaffold 104

Figure 5

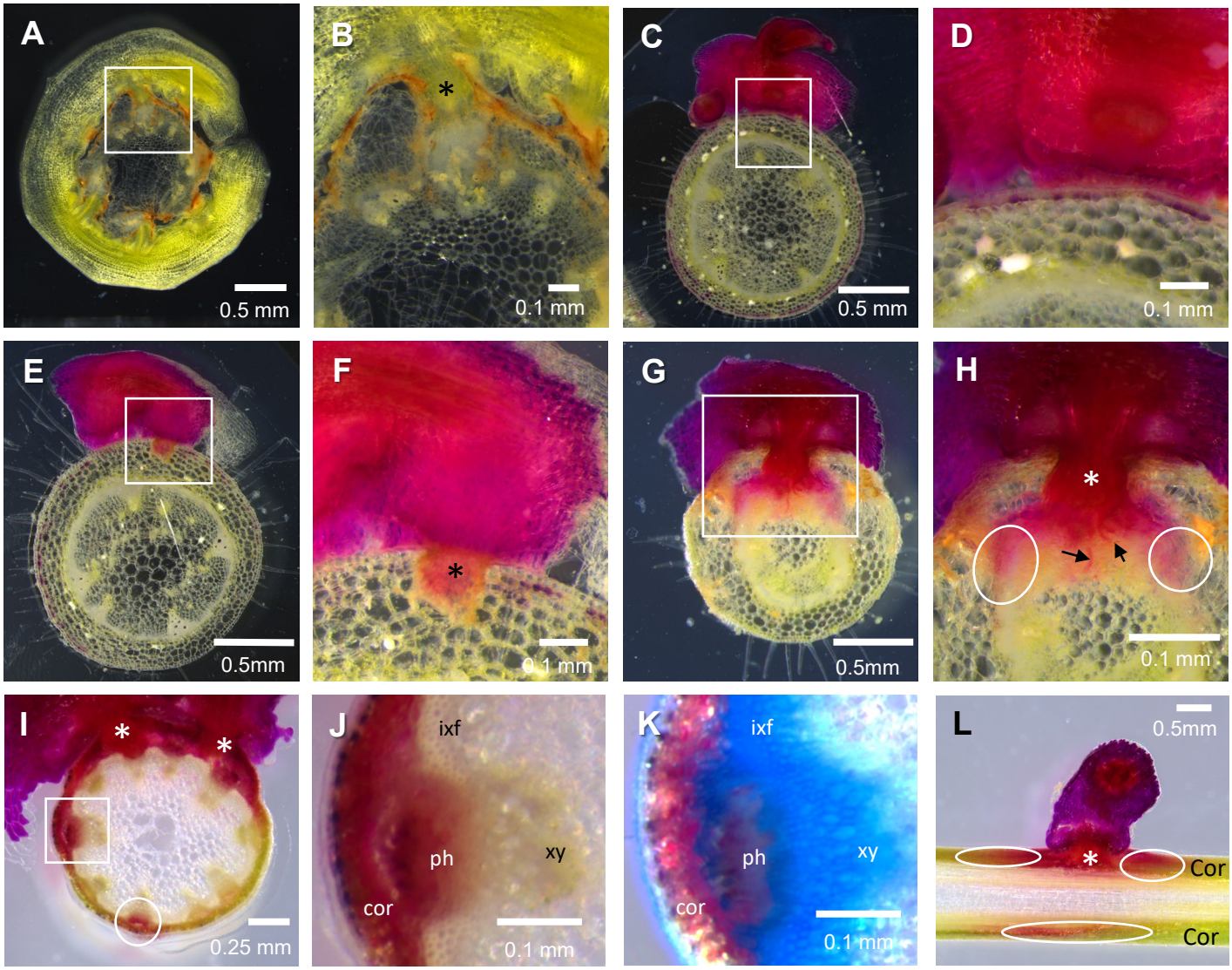
A
0.5 mm
B
*
0.1 mm
C
0.5 mm
D
0.1 mm
E
0.5mm
F
*
0.1 mm
G
0.5mm
H
*
0.1 mm
I
*
*
0.25 mm
J
ixf
ph
xy
cor
0.1 mm
K
ixf
ph
xy
cor
0.1 mm
L
0.5mm
*
Cor
Cor

Figure 6

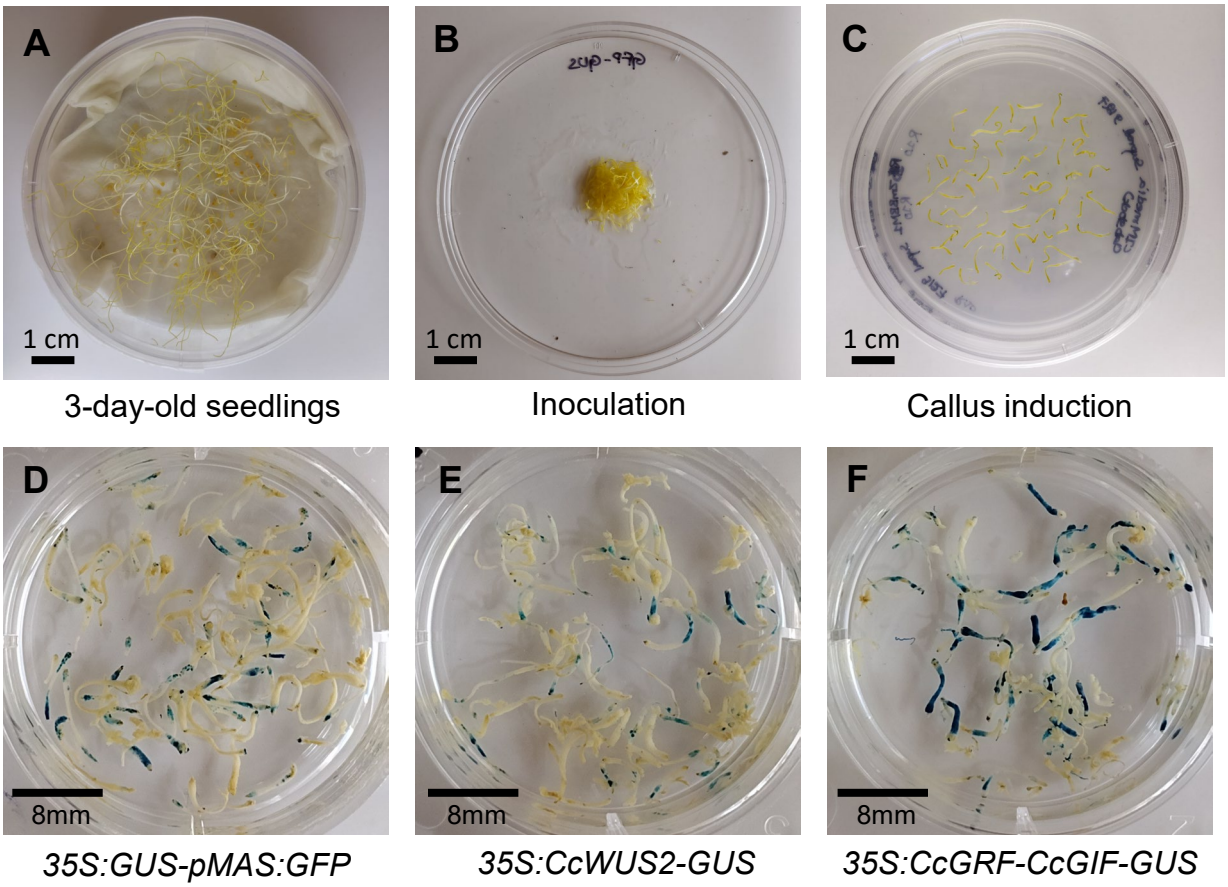
A
1 cm
3-day-old seedlings
B
1 cm
Inoculation
C
1 cm
Callus induction
D
8mm
35S:GUS-pMAS:GFP
E
8mm
35S:CcWUS2-GUS
F
8mm
35S:CcGRF-CcGIF-GUS

Figure 7

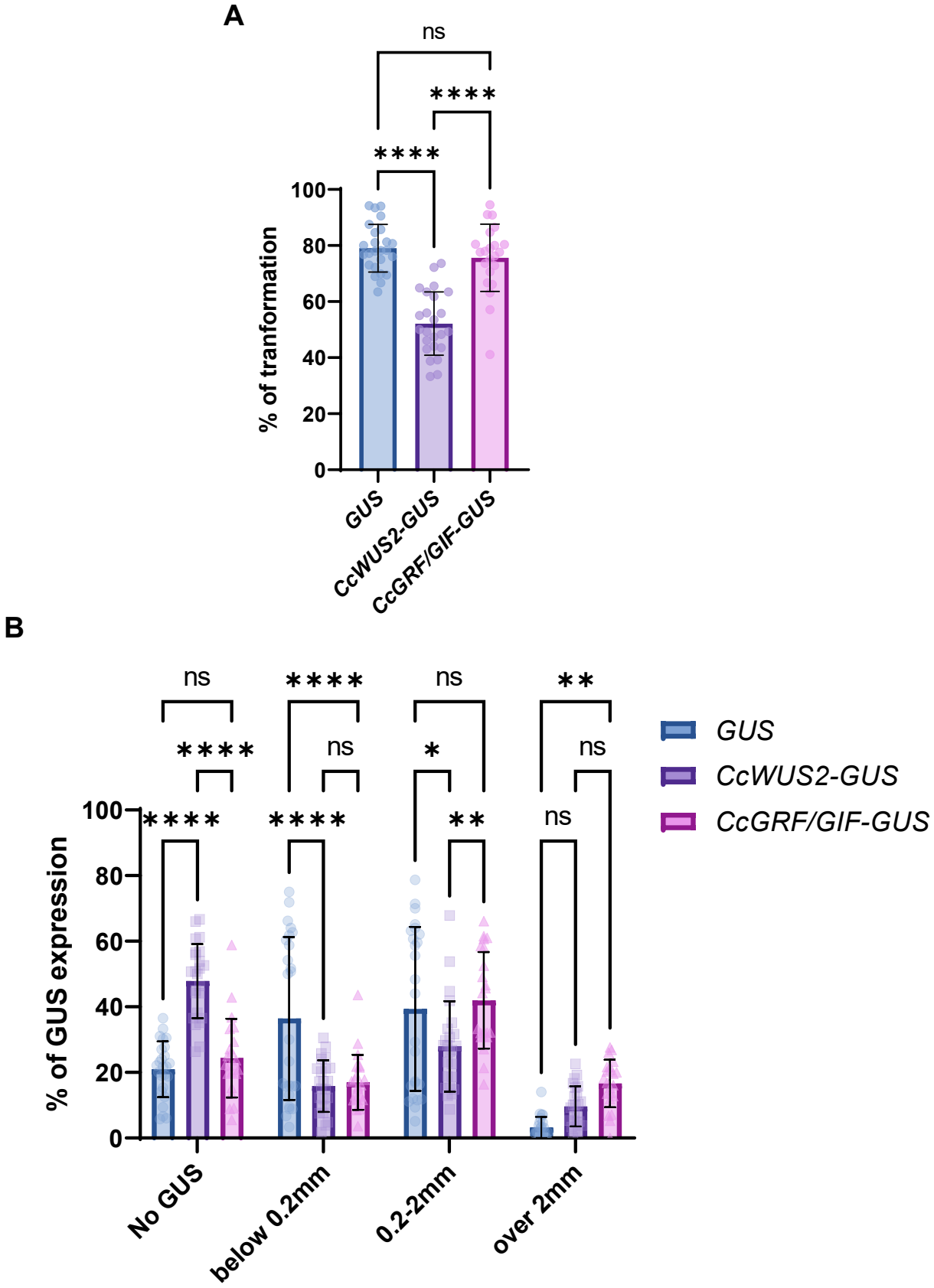
A
ns
****
****
100
80
60
40
20
0
% of tranformation
GUS
CcWUS2-GUS
CcGRF/GIF-GUS
B
ns
****
ns
**
****
ns
*
ns
****
****
**
ns
100
80
60
40
20
0
% of GUS expression
No GUS
below 0.2mm
0.2-2mm
over 2mm
GUS
CcWUS2-GUS
CcGRF/GIF-GUS

Figure 8

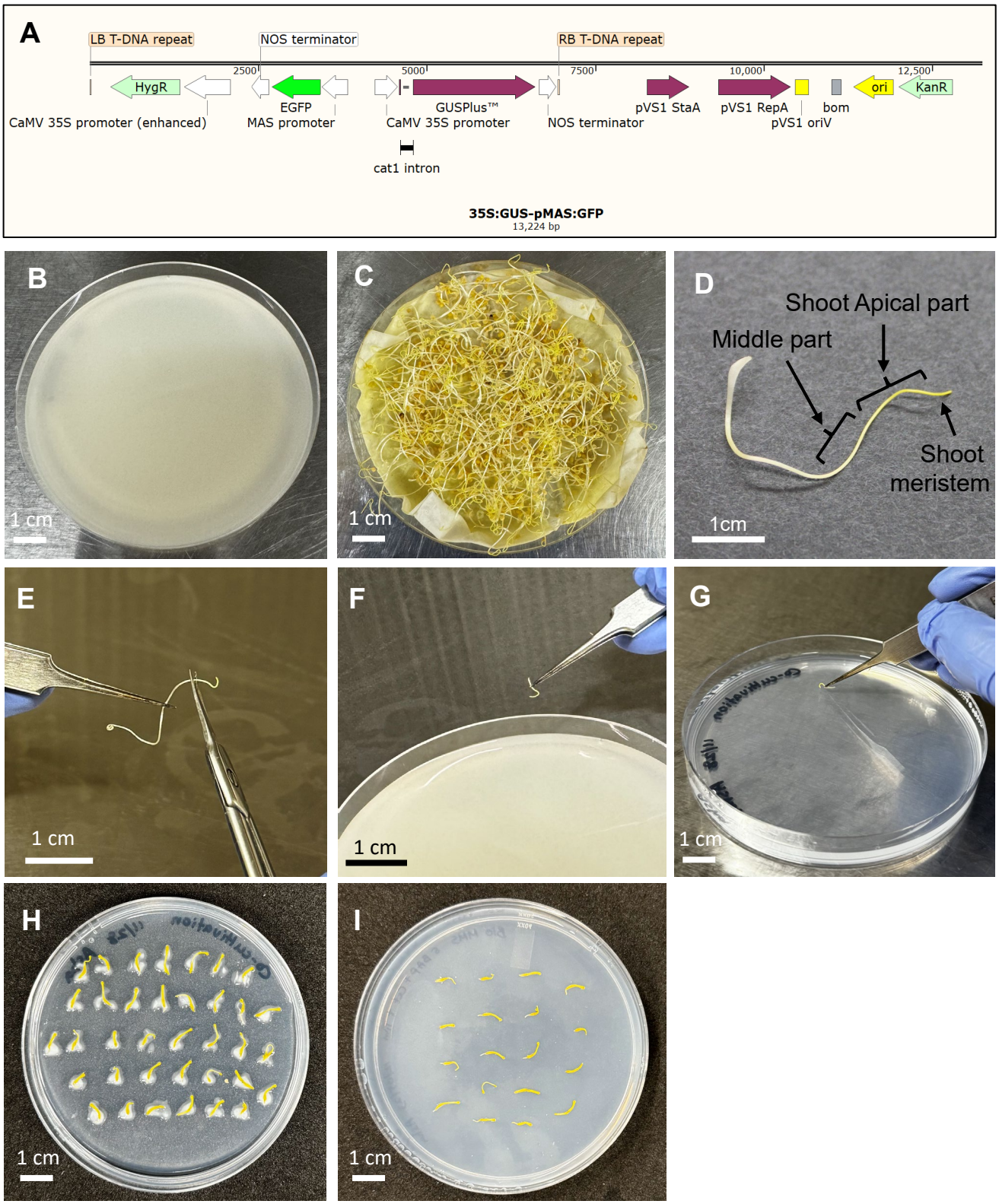

Supp Figure 1

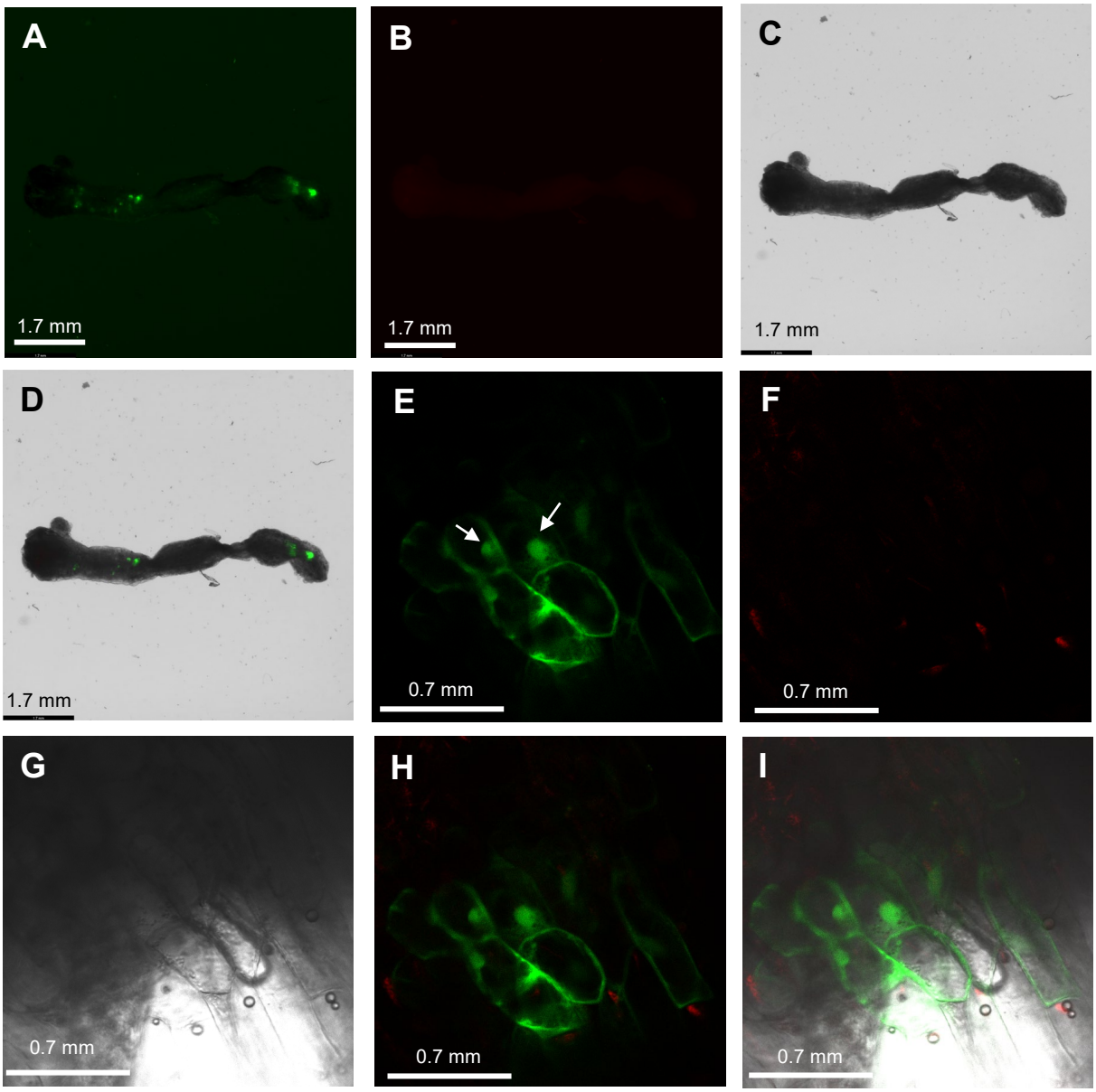

Supp Figure 2

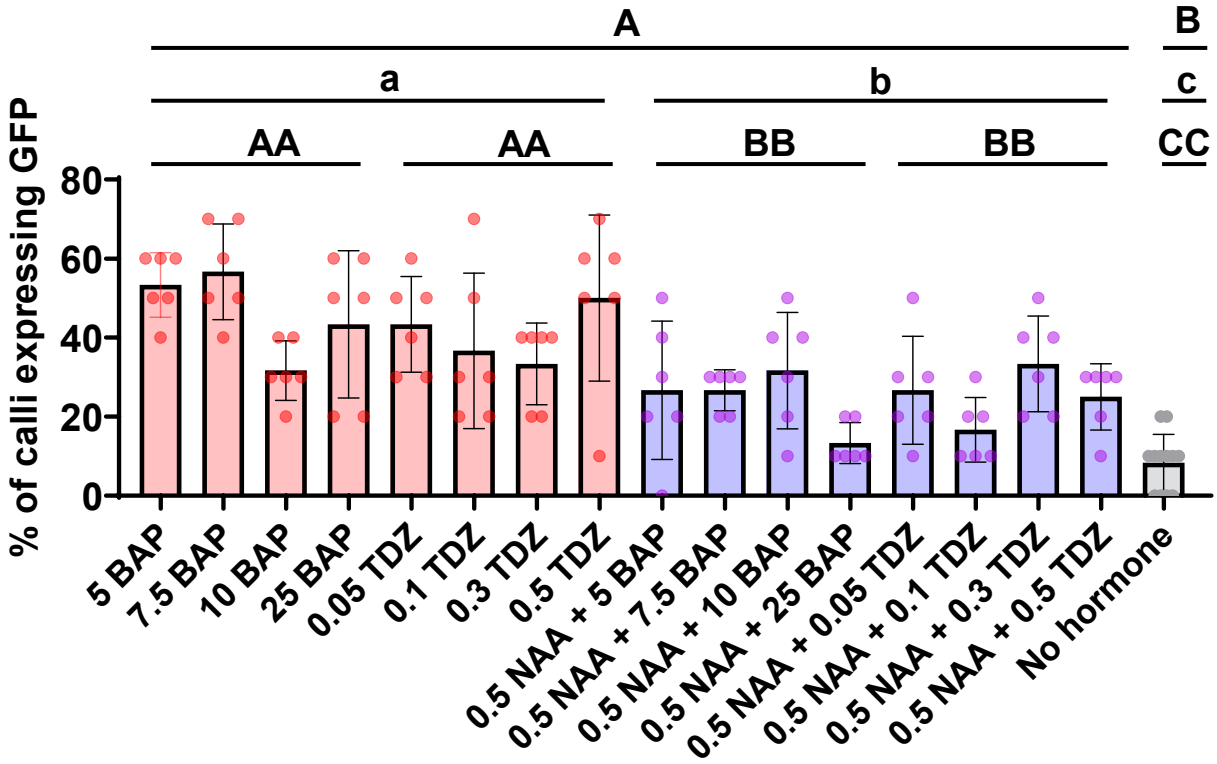

Supp Figure 3

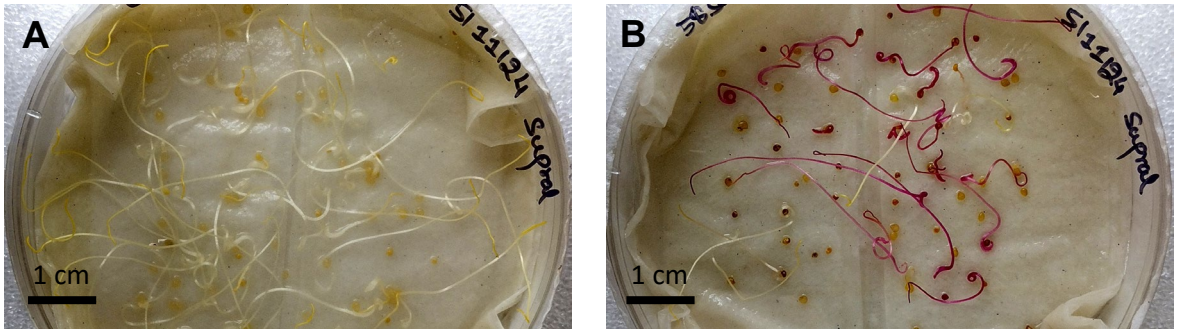

C. campestris

T1 transgenic *Cuscuta* *35S:RUBY* No. #11

Supp Figure 4

35S promoter and scaffolds 32B

ATGCTCCTCGTGGGTGGGGGTCCATCTTTGGGACCACTGTCGGCAGAGGCATCTTGAAC
GATAGCCTTTCCTTTATCGCAATGATGGCATTTGTAGGTGCCACCTTCCTTTTCTACTGTCC
TTTTGATGAAGTGACAGATAGCTGGGCAATGGAATCCGAGGAGGTTTCCCGATATTACCCT
TTGTAGAAAAGTCTCAAATCATCCATATATTCGATTGATTCTTTGCAGTACCCTTACCCGAC
TTATGGTGATACTTTATCTTCTAAAGGATTTCATATTCTCAGTGAGAATATGAAACGATCCA
AACGTACGAGACTTCCGACAACTTCTATGGATGTTATTTCACATTATCATCCTACAACAATT
CAAGTTGATAGCATTCCAATCGATCGCCAAATCTCTATCGGGTCAATCAACTAGCCCTTTG
ATCGCCTTCTTATTGGCCCTATCTGGGTGGACCCCTTCTGACCAGTCGTTCATCCCTCCGT
GGCGCGGCACACTTGTCCTACCGTCACCGAGTCAAGTCCCAAGCTGGTTAGCCATGGGTT
TACACCCATCACTTGGTACCCAATCTGGTGTGATTATTTGATATTGTTCTTATTTTTGTACTC
CCTACATCCTATTAGGACTTTCCAAATTCAAAGAAAAAATGTGTTGTCTATTATTTTTTCTCA
ATAATGAAATTTAATCACACTCTTC

35S promoter and scaffolds 104

ATGCTCCTCGTGGGTGGGGGTCCATCTTTGGGACCACTGTCGGCAGAGGCATCTTGGAC
GATAGCCTTTCCTTTATCGCAATGATGGCATTTGTAGGTGCCACCTTCCTTTTCTACTGTCC
TTTTGATGAAGTGACAGATAGCTGGGCAATGGAATCCGAGGAGGTTTCCCGATATTACCCT
ATCCATGAAACTTAGGAGTTCGCACCCCGCAGTTTCGTCCACCATTTGATCTGGACTGGG
GAGGGGGTATGAATCCATTGGACAAGCCTTGTTCAAGTCCGTATAATCCACACACATTCTC
CACGTGTCGCCCTTGGGAGCAAGGACAACGTTGGCCAGCCAATCCGGGTACTTGACTTC
CCGGATGTGACCAACACTGAGGAGGTCTCTCACTTCCTTCTTGACGAAGTCTCGCCGGTC
ACTCGCCAGGTACCGCTTCTTTTGGCGTACCGGTCGACTTCCCTCCCTCACGGCCAACCG
GTGGCAGATAACAGAGCGATCTATCCCGGGCATATCCGCCACGCTCCATGCGAATATGCC
CGCGTATTCTTGGAGGACCCGTGTAATCTGCTCCTTGAGATCCTCGGGAAGATTTGCTCC
AATTCTGACCATCCTCGAAGAATCACCCGGGTGAAGTTCGATTTCCACCGTCTCAGCCTC
GGGCTCTAGTTTCTCCTGGGTCTCTCCCTTGGTGATCTCTTGGGAGATGACATCGACCCC
CCTGGTCATTTTCTTGACTGCCCGGGCATAGCACTCCCGGGCGTTCCTCTGGTCGCCCTT
CATCTCACTCGACCA

Supp Figure 5

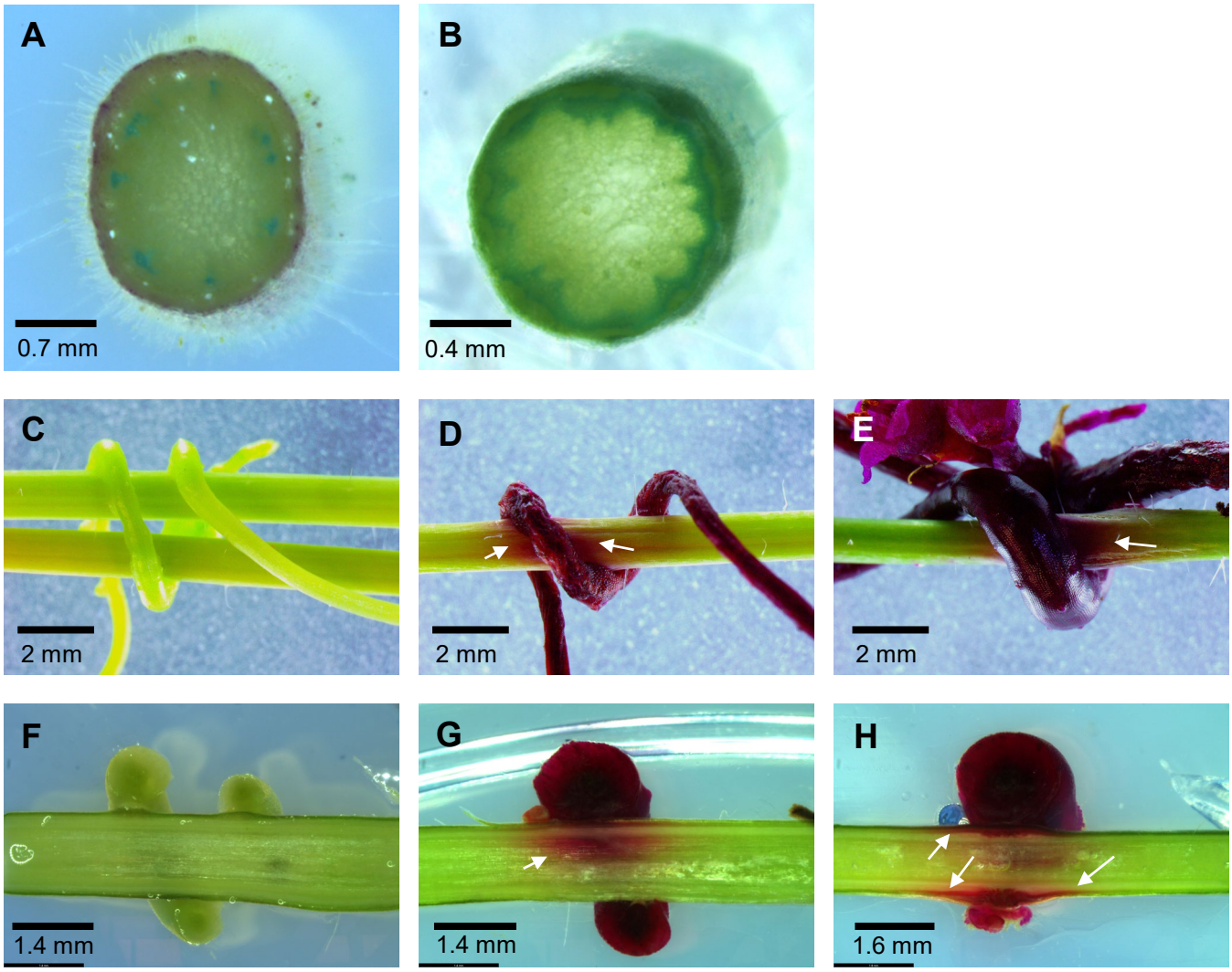

Supp Figure 6

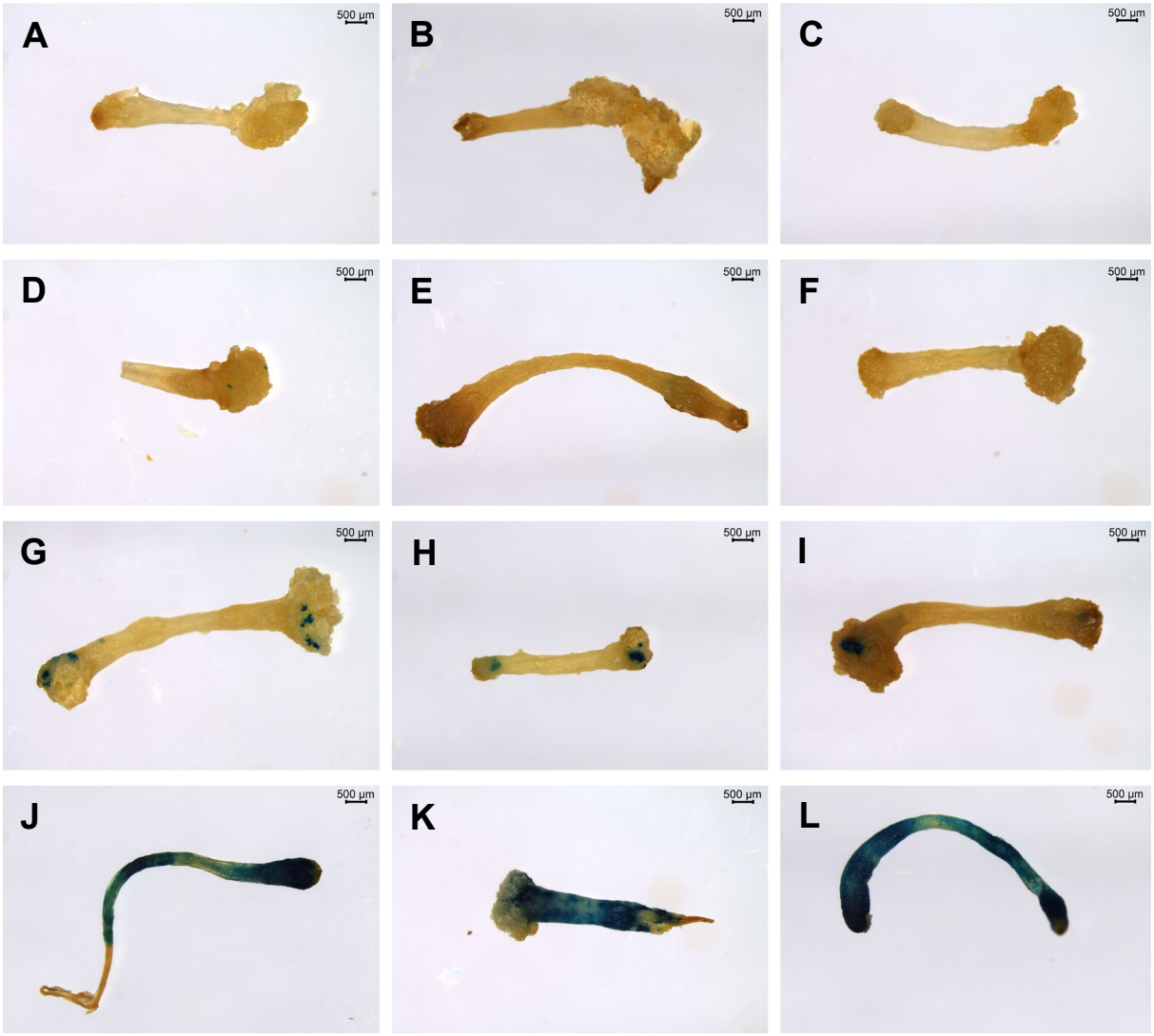

Supp Figure 7